An optical microscopy method for determining stable and metastable phase equilibria involving gas hydrate and ice: Application to CO2 + water systems

Abdelhafid Touil, Daniel Broseta

Journal Pre-proof

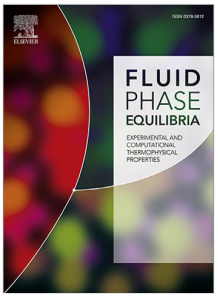

An optical microscopy method for determining stable and metastable phase equilibria involving gas hydrate and ice: Application to CO_2+water systems

Abdelhafid Touil, Daniel Broseta

PII: S0378-3812(25)00039-1
DOI: https://doi.org/10.1016/j.fluid.2025.114369
Reference: FLUID 114369

To appear in: *Fluid Phase Equilibria*

Received date : 3 October 2024
Revised date : 11 January 2025
Accepted date : 6 February 2025

Please cite this article as: A. Touil and D. Broseta, An optical microscopy method for determining stable and metastable phase equilibria involving gas hydrate and ice: Application to CO_2+water systems, *Fluid Phase Equilibria* (2025), doi: https://doi.org/10.1016/j.fluid.2025.114369.

Graphical Abstract

An optical microscopy method for determining stable and metastable phase equilibria involving gas hydrate and ice: application to CO_2+water systems.

Abdelhafid Touil, Daniel Broseta

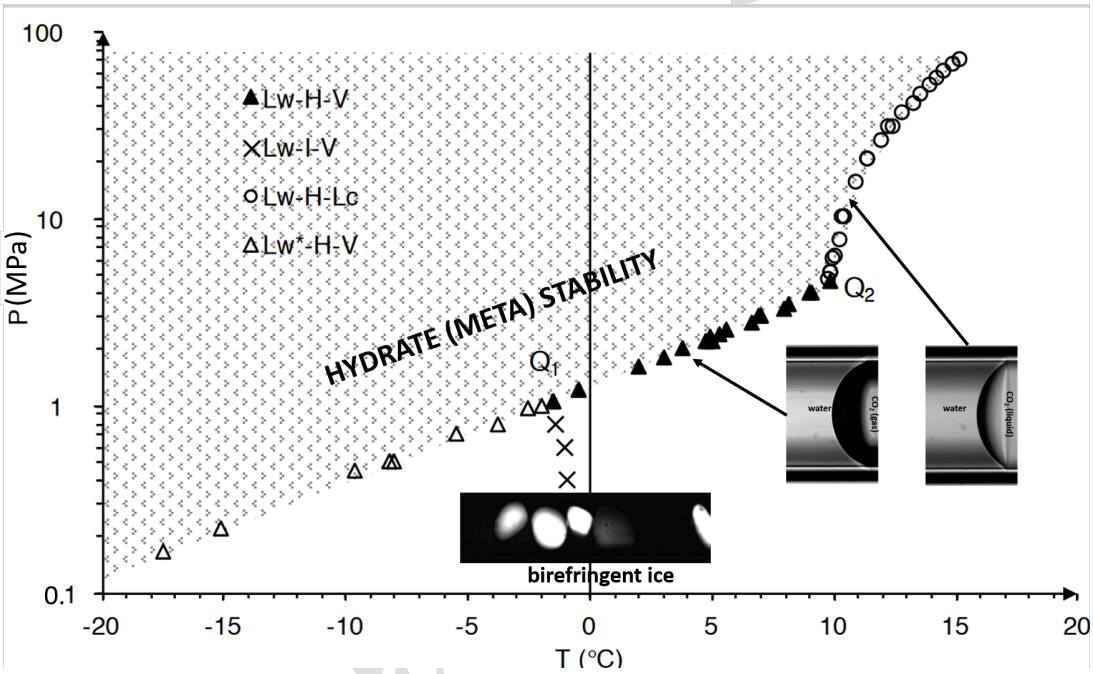

Highlights

An optical microscopy method for determining stable and metastable phase equilibria involving gas hydrate and ice: application to CO_2+water systems.

Abdelhafid Touil, Daniel Broseta

- An optical method is devised for the rapid determination of phase diagrams of water+hydrate-former systems.
- The method involves a transmission optical microscope and a thin cylindrical glass capillary used as an optical cell.
- The ice and/or gas hydrate crystals grow or shrink near the water/guest interface (meniscus) under controlled temperature and/or pressure.
- The birefringent ice and isotropic hydrate are discriminated by using crossed polarizers, and the liquid and vapor phases from their refraction effects.
- Three-phase lines involving ice or gas hydrate and two other fluid phases are determined, together with their intersections or quadruple points.
- The method is implemented with the water+CO_2 system, and the measured triple lines and quadruple points are in close agreement with the literature data.

An optical microscopy method for determining stable and metastable phase equilibria involving gas hydrate and ice: application to CO_2+water systems.

Abdelhafid Touil[a,b], Daniel Broseta[a]

[a] *Universite de Pau et des Pays de l'Adour, E2S UPPA, CNRS, LFCR, Pau, France*
[b] *Sonatrach, Direction Centrale Recherche et Developpement, Boumerdes, 35000, Algeria*

Abstract

The temperatures and pressures of the three-phase equilibria between liquid water (L_w), gas hydrate (H) and a guest-rich phase (a vapor, V, or a condensed liquid, L_c) and between L_w, ice (I), and V, are determined experimentally by monitoring the disappearance of the hydrate or ice phases near the meniscus between the water-rich and guest-rich phases when temperature or pressure are varied slowly. This monitoring is carried out by optical microscopy used in the transmission mode with or without crossed polarizers, the latter serving to identify the presence or absence of hexagonal (birefringent) ice. The guest molecule (or hydrate-former) taken as an example is CO_2. The triple lines corresponding to L_w-H-V, L_w-I-V and L_w-H-L_c equilibria are determined together with their intersections, i.e., the lower quadruple point Q_1 (L_w-I-H-V coexistence) and upper quadruple point Q_2 (L_w-H-V-L_c coexistence).The metastable extension of the three-phase line L_w-H-V for temperatures and pressures below those of Q_1 is also determined. A Clausius-Clapeyron treatment of this line and its metastable extension shows that a similar dissociation process exists, whether the dissociation is to supercooled liquid water or not.

Keywords: CO_2 hydrate, phase diagram, quadruple points, three-phase lines, Clausius-Clapeyron, heat of hydrate dissociation, self-preservation

Email addresses: abdelhafid.touil@sonatrach.dz (Abdelhafid Touil), daniel.broseta@univ-pau.fr (Daniel Broseta)

1. Introduction

A large research effort is being devoted to the determination of hydrate phase equilibria, which must be known precisely for many applications, whether the hydrate is to be avoided (e.g., in the transport of wet gases) or promoted (e.g., for gas separation and storage, secondary refrigeration or water treatment processes) [1]. Phase diagrams of two-component systems (here, water and the hydrate-former – or guest molecule) are conveniently described by three-phase equilibrium lines, which delineate regions of two-phase coexistence in the temperature and pressure (T and P) plane. One of these lines, the hydrate dissociation line, corresponds to the equilibria between the hydrate phase (H), the aqueous liquid phase (L_w) and the guest-rich phase, which itself may be either a liquid (L) or a vapor (V). The ice dissociation line is another three-phase line of interest, which occurs at relatively low pressures and temperatures (in the range of 0°C) and corresponds to the equilibria between ice (I), the aqueous (L_w) and guest-rich vapor (V) phases. These two lines meet at the lower quadruple point usually noted Q_1, where the ice (I), the hydrate (H), the aqueous (L_w) and vapor (V) phases coexist; the temperature of Q_1 is close to the ice melting temperature (0°C). When under higher temperatures and pressures than those of Q_1, the guest-rich phase undergoes a transition from a vapor (V) to a condensed liquid (L_c), there also exists an upper quadruple point (noted Q_2) where the hydrate coexists with an aqueous phase (L_w) and the guest-rich liquid and vapor phases (L_c and V).

The appearance (or nucleation) of a novel phase in a fluid system requires conditions that may strongly depart from equilibrium conditions, especially when the system occupies a small volume. This departure is the driving force for the nucleation and subsequent growth of this novel phase. For the systems of interest here, it is often given by the supercooling (or subcooling) T_{eq}-T, the difference between T, the temperature of the experiment, and T_{eq}, the three-phase equilibrium temperature at the pressure of the experiment, or by P-P_{eq}, where P is the experimental pressure and P_{eq} the equilibrium pressure at the temperature of the experiment. For volumes in the micro- to nano-liter range, subcoolings in the range of 30-40°C are typically required for the primary nucleation of ice or gas hydrate [2]. Unlike its appearance, the disappearance of the novel phase takes place without any hysteresis: the three-phase equilibrium conditions are obtained by letting the novel phase, here the ice or gas hydrate, disappear in presence of the other (fluid) phases

under a slow increase in T or slow decrease in P.

We report in this paper an optical microscopy determination of phase diagrams of a two-component system, water and a small molecule (CO_2), with up to four different phases: a liquid (water-rich) phase (L_w), gas hydrate (H), ice (I) and a non-aqueous, guest-rich (CO_2-rich) phase, either vapor or liquid (V or L_c). Attention is paid to the hydrate dissociation line and the point on this line where the coexisting guest-rich phase changes from vapor (V) to liquid (L_c): this is the upper quadruple point Q_2. The ice dissociation (I-H-V) line is also determined, which intersects the hydrate dissociation (L_w-H-V) line at the lower quadruple point Q_1. We also explore the metastable extension of the latter line to conditions where the liquid water phase is supercooled, i.e., to temperatures and pressures below those of the quadruple point Q_1. This extension (noted L_w*-H-V) is believed to have some connection with the phenomenon of gas hydrate self-preservation, which describes long-lived (strongly metastable) gas hydrates outside their stability domain – under low pressures and temperatures below 0°C or, more precisely, below the temperature and pressure of the lower quadruple point Q_1 [3].

The interest of choosing CO_2 and water for implementing the proposed method of phase diagram determination is that its three-phase equilibrium lines (triple lines) and their intersections – the quadruple points Q_1 and Q_2 – have already been determined by a variety of experimental methods and are available in the literature, thus allowing a proper test of the proposed method. A compilation of the literature data acquired prior to 2007 can be found in Sloan's book [4]. For the sake of simplicity only the data published since 2007 are considered here, as these data are focused on the features addressed in this work, namely the triple line involving supercooled water (L_w*-H-V) [3] and some of the other triple lines and their intersections [5, 6, 7, 8], i.e., the quadruple points Q_1 and Q_2, which can also be determined directly [9]. A thorough literature review of three- and four-phase equilibria in CO_2+H_2O binary systems can be found in the latter, very recent reference [9].

The outline of this paper is as follows. The experimental setup and procedure are described in next section. The setup involves a thin cylindrical glass capillary used as an optical cell initially filled with water and the guest phase (CO_2) separated by a meniscus, similar to the one described in our previous work [2] and in other recent investigations [8, 10, 11]. The interest of using thin glass capillaries is the very rapid equilibrium time when the temperature of the heating/cooling stage is changed – less than a few tens of

seconds. The focus is on the meniscus region, where the gas hydrate or ice crystals are observed to grow or shrink on one side of the interface. Those two solid phases may be difficult to distinguish by using solely transmission optical microscopy [8]. The novelty here is that the transmission optical microscope is used also with crossed polarizers, which allows to discriminate the (isotropic) hydrate from the (birefringent) hexagonal ice, the prevalent ice crystal structure for the temperatures and pressures of interest. Then, the following sections present and discuss the results for the triple lines — including the metastable extension of the hydrate dissociation line — and the quadruple points Q_1 and Q_2. It also presents and discusses the heats of dissociation of the CO_2 hydrate as inferred from the hydrate dissociation line and its metastable extension below the quadruple point Q_1. The last section is devoted to the Conclusions and Perspectives.

2. Experimental setup and procedures

The experimental setup has been described in detail in ref. [2]. The optical (observation) cell is a 10 cm-long cylindrical glass capillary (200/330 µm ID/OD, Vitrotubes), filled with 1-2 cm of deionized water against the sealed end of the capillary, whereas the open end is glued into a 1/16" stainless steel tube, itself connected to a three-way valve (Topindustrie) and an ISCO DM65 syringe pump that contains the guest (CO_2 from Linde, with purity 99.995%) and is used in the pressure-controlled mode up to 10 000 psi (69 MPa). In addition to the sensor of the pump, pressures below 30 MPa are also monitored with a Keller (LEO2) digital manometer installed along the steel tube. The capillary is installed in a cooling/heating stage (Linkam CAP500) allowing it to be displaced along the two horizontal directions, and equipped with temperature control to ± 0.1 K (with the LINKSYS software) on an Olympus BX50 upright microscope stand, with a x10 extra-long working distance objective (Olympus) and a Ueye UI 3360 Camera run at one frame per second. The temperature sensor is calibrated against the ice point, using a glass capillary initially loaded with pure water. The estimated uncertainty of the measured temperatures is therefore twice 0.1 K,, i.e., ± 0.2 K. As to the pressure, the uncertainty is estimated to be ± 0.03 MPa for pressures lower than 30 MPa (0.1% of the full scale of the LEO2 manometer as given by the manufacturer) and 0.34 MPa above 30 MPa (0.5% of the full scale of the manometer of the ISCO DM65 pump as given by the manufacturer).

The observations with the optical microscope are focused on the interface

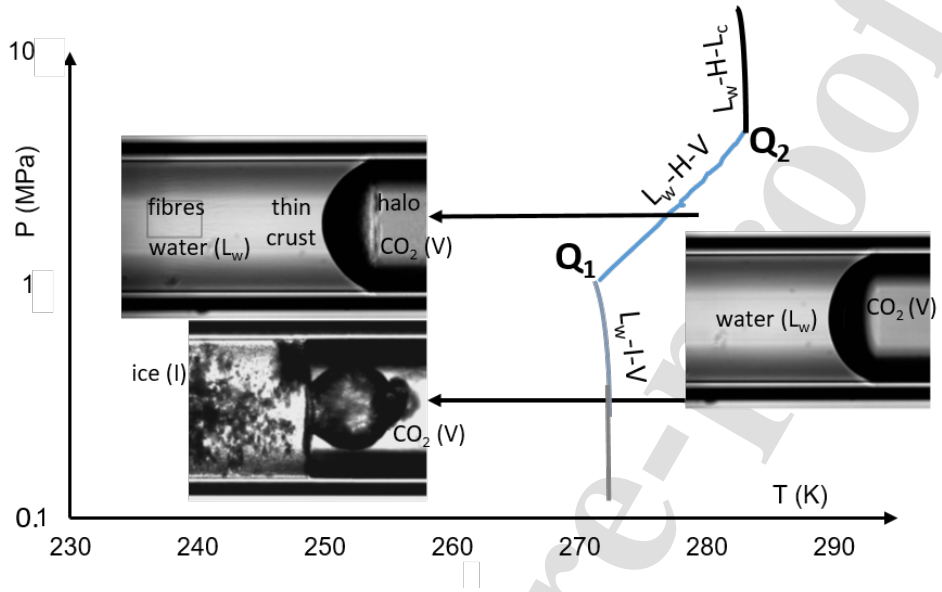

Figure 1: Primary hydrate formation upon cooling. Snapshots of the water-CO_2 meniscus region in a glass capillary (ID $\approx$ 200 µm) at the start of the experiment (T close to the ambient) and right after primary ice or hydrate formation by driving the capillary to low enough T. Under low pressure all the water freezes into ice, whereas under higher pressure the hydrate nucleates and spreads on the water/guest meniscus and as a halo on the substrate, with hydrate fibres growing into the water phase. Note the important refraction effects near the glass wall with gaseous CO_2. Owing to the small fluid volumes, nucleation occurs tens of K below the equilibrium temperature.

separating the water- and guest-rich phases, a spherical meniscus at the start of the experiment (T close to the ambient). The experiment starts with the primary (or first) formation of the solid phase(s), gas hydrate and/or ice, which is obtained by lowering the temperature under constant pressure, typically tens of °C below the equilibrium temperature (see [2] and Figure 1). Under low pressure – a few bar – the phase that nucleates first upon cooling is ice: all the liquid water present is almost instantly converted into ice, which has a very characteristic dotted texture (dots are gas inclusions) and bulges out the middle of the meniscus [2, 12]. The positions of the water/guest and ice/water menisci are significantly different, as ice occupies a larger volume than liquid water. Under high enough pressure (above a few bar in the case of CO_2 hydrate), the hydrate is the solid phase that nucleates

first upon cooling, followed by ice if the temperature descent is not stopped. The hydrate phase rapidly spreads as a thin polycrystalline hydrate crust on the meniscus, and then beyond the contact line as a halo on the glass wall of the capillary. Figure 1 provides an illustration of the CO_2 hydrate formed on and around the meniscus shortly (less than 1 s) following primary nucleation; simultaneously, gas hydrate fibres or dendrites expand from the hydrate crust into bulk water, whose detection may require high-resolution microscopy methods (the refractive indices of CO_2 hydrate and liquid water are very similar) (see [2]).

As soon the gas hydrate is detected, the temperature descent is stopped. To avoid ice formation, temperature is raised, while keeping the pressure constant. The dissociation (equilibrium) temperature for that pressure is then determined by a temperature-search method, which is detailed in next section.

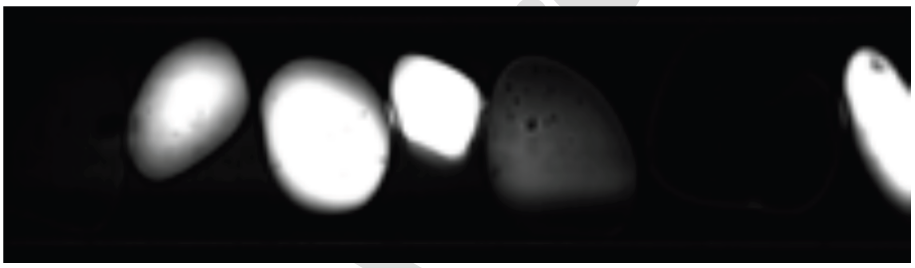

Figure 2: Observation under crossed polarizers of disk-shaped crystals of hexagonal ice in liquid water at 271.6 K and gaseous CO_2 (0.6 MPa), featuring their birefringent character.

To assess the presence (or absence) of ice, the transmission microscope is used with crossed polarizers, that is, by setting a polarizer and analyser on both sides of the sample to extinguish all transmitted light but that crossing a birefringent material, here hexagonal ice (noted I in this study). Situations where both ice and the hydrate phases coexist are avoided in this study.

With hydrate formers such as CO_2, the guest-rich phase may be either liquid or gaseous, depending on temperature and pressure. The nature of that phase is identified from the respectively weak and strong refraction effects: a gaseous (low-refractive-index) phase generates a marked darkening close to the meniscus and near the walls of the cylindrical capillary (see Figure 3).

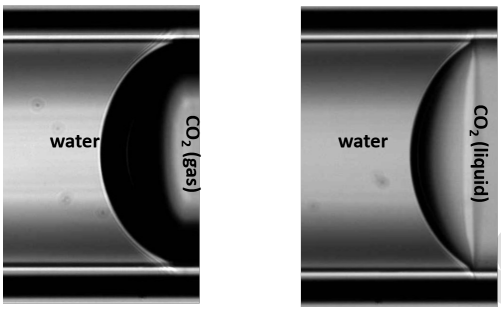

Figure 3: Meniscus between liquid water and CO_2, either liquid (left) or gaseous (right), observed by transmission optical microscopy. Because of its low refractive index, gaseous CO_2 looks darker than in the region near the meniscus and capillary walls.

3. Results and discussion

3.1. The hydrate dissociation lines: L_w-H-V and L_w-H-L_c equilibria

The optical microscope is used in the transmission mode, and the crossed polarizers are used only to check the absence of ice. For a (high enough) pressure P such that the CO_2 hydrate has been formed on the meniscus (first formation, see above), temperature is raised as soon as the hydrate is detected, to a value such that the hydrate starts melting. The equilibrium temperature at that pressure $T_{eq}(P)$ is approached by sequences of stepwise temperature increases (in order to shrink and eventually melt the hydrate crystals) and decreases (to regrow the hydrate crystals or reform them by virtue of the memory effect), carried out under increasingly lower rates (Figure 4). The interval between the dissociation and reformation temperatures is lowered until one (or very few) hydrate crystal(s) is (are) observed to diminish very slowly in size at a given temperature, and grow very slowly 0.1 K below that temperature, then considered to be the equilibrium temperature $T_{eq}(P)$. (The measurement uncertainty on $T_{eq}(P)$ is estimated to be equal to 0.1 K plus the uncertainty in the calibration of the temperature sensor, another 0.1 K.) Then, by changing the imposed pressure, a new equilibrium temperature T_{eq} is obtained, etc.

A set of a dozen of equilibrium points is obtained within a working day. The experimental values determined in this study are listed in Appendix A. The L_w-H-V equilibria obtained in this study are displayed in Figure 5, together with recent literature data.

The temperatures and pressures of L_w-H-V equilibria are also displayed

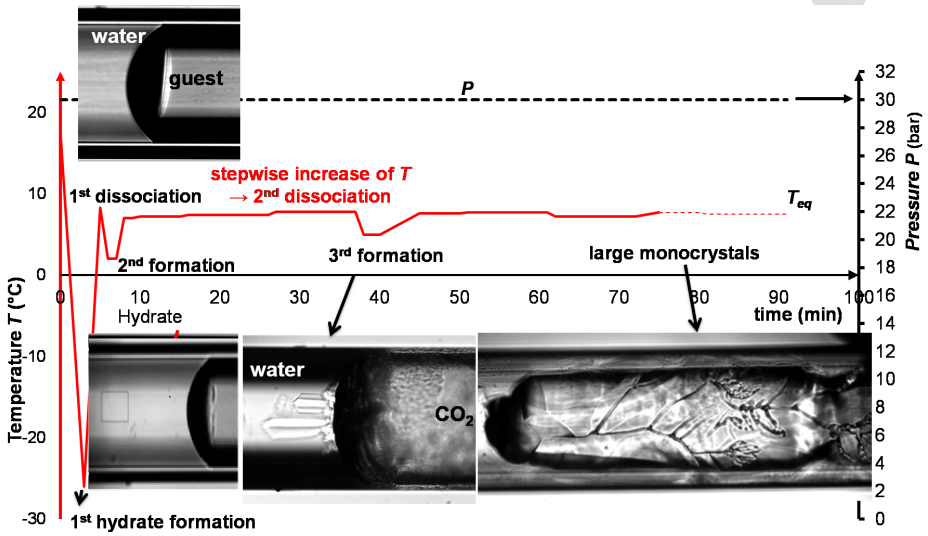

Figure 4: Determination of the dissociation temperature T_{eq} at a given P through a sequence of stepwise temperature variations around T_{eq}, starting from a water/guest spherical meniscus at ambient temperature. The morphology of the hydrate crystals depends on subcooling, e.g., there are large monocrystals under low subcooling (or distance to T_{eq}).

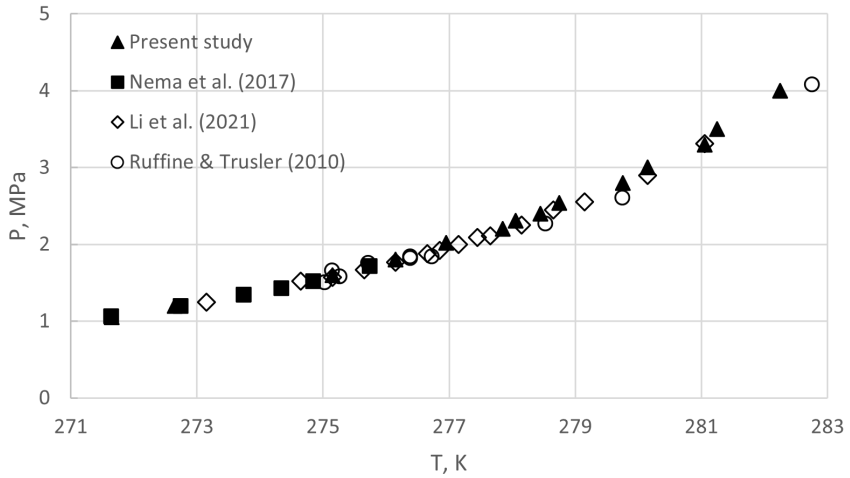

Figure 5: Temperatures and pressures of the L_w-H-V equilibria of the CO_2+H_2O binary system, with data points from the present study, Ruffine and Trusler [6], Nema et al. [7] and Li et al. [13].

Figure 6: Semi-logarithmic plot of the temperatures and pressures of L_w-H-V and L_w-H-L_c equilibria of the CO_2+H_2O binary system, with data points from this study, from Ruffine and Trusler [6] and Ohgaki et al. [14]. The two lines meet at the quadruple point Q_2.

together with those of the L_w-H-L_c equilibria in Figure 6 in semi-logarithmic coordinates to highlight the angular point that delineates the two lines - the upper quadruple point Q_2. Its coordinates are T_{Q_2}=282.95 K and P_{Q_2}=4.47 MPa, in accord with those determined by Ruffine and Trusler (282.85 K and 4.43 MPa) [6].

3.2. Metastable extension of the hydrate dissociation line: L_w^*-H-V equilibria

The extension of the hydrate dissociation line L_w-H-V to conditions where the hydrate is in equilibrium with supercooled water (L_w^*) is obtained by a modification of the experimental procedure described above. Following the primary formation of hydrate (by cooling the sample under high enough pressure), temperature is raised to below 273 K or 0°C (to -15°C or 258 K in the example of Figure 7) while pressure is decreased as well (to 5 bar or 0.5 MPa in the example of Figure 7) and then kept constant. The temperature-search method described above is then used to locate the temperature of the L_w^*-H-V equilibrium at that pressure P. Remarkably, and even though temperature is well below the ice point (0°C), the gas hydrate melts to liquid

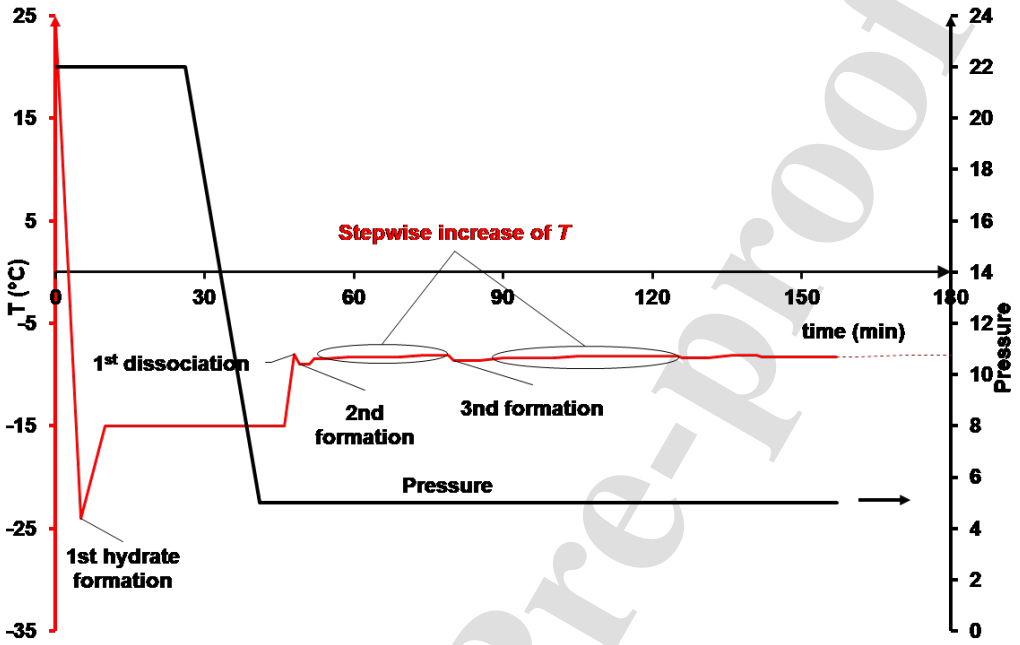

Figure 7: Procedure for determining equilibria between gas hydrate, vapor and supercooled water.

water (it does not convert into ice) and vice-versa the liquid water turns into a gas hydrate phase (and not into ice) when temperature is driven back and forth across the temperature of the L_w^*-H-V equilibrium at that pressure P. The same phenomena that occur at temperatures above 0°C (see above) also occur with the supercooled water + gas system: in particular, hydrate monocrystals are also observed to form under very small subcoolings (data not shown). Once the equilibrium temperature is determined, pressure is changed and the temperature of the new L_w^*-H-V equilibrium is determined, etc. Over the time spent (in the order of one day) to determine the whole L_w*-H-V line down to temperatures in the range of 253 K, the aqueous phase remains a supercooled liquid, with no indication of ice formation – no bulk freezing of the liquid water compartment (the absence of ice is checked by means of the crossed polarizers). As a matter of fact, water remains a supercooled liquid under temperatures well below its freezing point, as it does in the absence of hydrate: this is due to the very small sample volumes

(well below the microliter), to which nucleation probability is proportional.

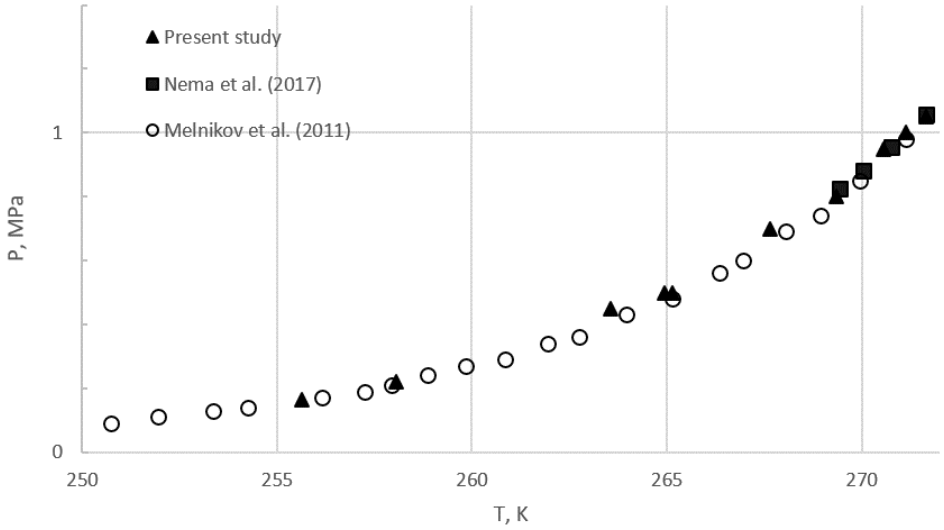

Figure 8: L_w^*-H-V equilibria between gas hydrate, vapor and supercooled water measured in this study and by Melnikov et al. [3] and Nema et al. [7].

The pressures and temperatures of the L_w^*-H-V equilibria measured in this study are reported in Appendix A, and are displayed in graphical form in Figure 8, where they are compared to two sets of literature values. One set originates from observations of water droplets, with volumes slightly above the water volumes of this investigation [3]. The other set is obtained from experiments carried out with large volumes of water and gas (a few tens of cm^3) and therefore the temperature range of liquid water metastability below 0°C is limited [7].

3.3. Ice dissociation line: L_w-I-V equilibria.

The temperature of equilibrium between liquid water, ice and vapor for a given (low) pressure is determined by varying the temperature and observing the melting and reformation of ice near the water/vapor meniscus. Following the primary formation of ice (see Figure 1), thin disk-shaped ice monocrystals floating in water become apparent upon approaching 0°C (273.15 K). Those

thin plates are the most apparent when observed with crossed polarizers (Figure 2). They grow and shrink laterally (in the plane perpendicular to the c-axis of hexagonal ice) when temperature is respectively below and above the equilibrium temperatures. Four equilibria have been obtained, whose temperatures and pressures are listed in Appendix A and plotted in Figure 9.

3.4. Heats of hydrate dissociation to vapor and water. Coordinates of the quadruple point Q_1.

A semilogarithmic plot (Figure 9) of pressure P versus reciprocal absolute temperature 1/T for the pressures and temperatures shows that ln(P) varies linearly with 1/T along the dissociation line L_w-H-V and its metastable extensionL_w^*-H-V from the lowest temperature ($\approx$ 253 K) to the temperature of the upper quadruple point Q_2 ($\approx$ 283 K).

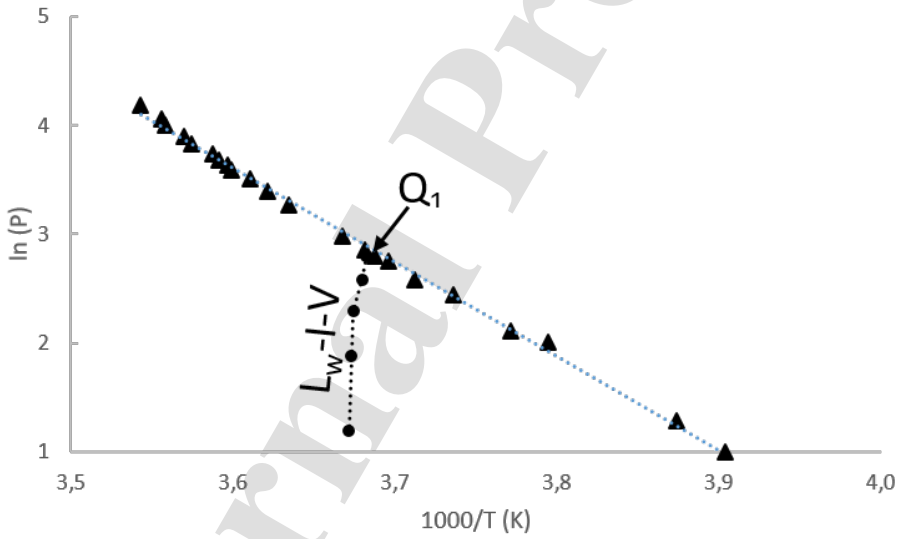

Figure 9: Experimental pressures P vs. reciprocal temperatures 1/T of the hydrate dissociation line (L_w-H-V) and its metastable extension (L_w^*-H-V) and the ice dissociation line and L_w-I-V (semi-logarithmic coordinates).

If the volume difference between the hydrate and meltwater is neglected, the Clausius-Clapeyron equation can be used. The slope characterizing the above linear behavior to ΔH is related to the heat of dissociation of hydrate per mole of gas liberated:

$$\frac{dln(P)}{d(1/T)} = \frac{-\Delta H}{ZR} \quad (1)$$

where R=8.3145 J/mol K is the gas constant and Z the compressibility factor of gaseous CO_2 at the pressure P and temperature T of interest, defined as PV/RT, where V is the volume of one mole of CO_2 at T and P.

The quantity $\Delta H/Z$ (i.e., the slope multiplied by R) extracted from the data plotted in Figure 9 is equal to 72 kJ/mole of gas (CO_2) liberated, to be compared with the value of 77 kJ/mol obtained by Ruffine and Trusler [6]. Z changes significantly along the hydrate dissociation line: from the values of V found in the NIST database (webbook.nist.gov/chemistry), $Z \approx 0.63$ at Q_2 and 0.92 at Q_1, which corresponds to dissociation heats respectively equal to 45.3 and 66.2 kJ per mole of CO_2 liberated.

When the ice dissociation line is plotted together with the hydrate dissociation line and its metastable extension, the intersection between the two lines (Figure 9) is nothing but the lower quadruple point Q_1, whose coordinates are determined here to be $T_{Q_1} \approx 271.55$ K and $P_{Q_1} \approx 1.04$ MPa. T_{Q_1} is 1.6 K lower than 273.15 K (or 0°C), which is an effect of the significant solubility of CO_2 in liquid water. It is the manifestation of the depression of the freezing point of a solvent (here, water) induced by a solute (here, CO_2), which increases linearly with the (low) solute molality (irrespective of the nature of the solute). The linearity coefficient for water is equal to 1.86 K/molal [15]: a value very close to 1.6 K is obtained when multiplying this coefficient by the molal concentration of CO_2 in water under T≈ -1.5°C and P≈ 1 MPa (about 0.83 mol/kg H_2O [16]).

These values of T_{Q_1} and P_{Q_1} are close to those inferred by Melnikov and coworkers [17] from observations of ice crystals in water droplets under a CO_2 atmosphere (T_{Q_1} ≈271.65 K and P_{Q_1} ≈1.03 MPa) and by Nema et al. [7] from the intersection between the hydrate dissociation line and the I-H-V (ice/hydrate/vapor) line [5] ($T_{Q_1} \approx 271.6$ K and P_{Q_1} ≈1.04 MPa). Recent direct measurements following the formation of the hydrate and ice phases in an initially two-phase gas–water system under intense agitation indicate that T_{Q_1} ≈271.6 K and P_{Q_1} ≈1.044 MPa [9].

4. Conclusions and perspectives

A simple experimental methodology has been devised and implemented with the water+CO_2 system, that allows the rapid and precise determination

of phase diagrams – particularly the three-phase lines and quadruple points – of two-component, water and hydrate former, systems. One working day suffices to measure over an extended range the temperatures and pressures of the three-phase lines, whether one of the phases is gas hydrate or ice. The three-phase lines and quadruple points measured for the water + CO_2 system by using this methodology are in close agreement with the available experimental values obtained by other methods.

The methodology uses a thin cylindrical glass capillary (with diameter below the mm), in which the water and hydrate-former phases separated by a meniscus are initially installed and driven to temperature and pressure conditions such that the gas hydrate and/or the ice phase(s) form. Temperature and/or pressure are then tuned to let the latter phase(s) near the meniscus either grow or vanish and approach the three-phase equilibrium conditions. An optical microscope used in the transmission mode with or without crossed polarizers helps discriminate (birefringent) hexagonal ice from (isotropic) gas hydrate. It should be effective not only with structure I hydrates such as the CO_2 hydrate considered in this study but also for structure II hydrates, which are isotropic crystals as well. The liquid or vapor nature of the non-aqueous (guest-rich) phase is assessed from the limited refraction effects when it is a liquid and pronounced effects when it is a vapor – giving rise to dark regions near curved interfaces.

In this study, situations where ice and gas hydrate coexist below 0°C have been avoided. Future work could/should examine such situations, particularly temperature and pression conditions near the H-I-V triple line. The method could also be extended to more complex hydrate-forming systems, such as those exhibiting three-phase envelopes rather than lines, where the compositions of the various phases could also be measured by means of micro-Raman spectroscopy.

5. Acknowledgement

This work has been partially supported by project ANR-22-PESP-0007, and has benefited from discussions with Patrick Bouriat, Ross Brown and Guilhem Hoareau.

Appendix A. Three-phase equilibria involving CO_2 hydrate, liquid water (supercooled, L_w^*, or not, L_w), ice (I) and the CO_2-rich phase (either vapor, V, or liquid, L_c).

L_w^* – H – V	
T (K)	P (MPa)
256.15	0.17
258.15	0.22
263.55	0.45
265.15	0.50
267.65	0.70
269.35	0.80
270.55	0.95
271.15	1.00

L_w – H – V	
T (K)	P (MPa)
271.65	1.05
272.65	1.20
275.15	1.60
276.15	1.80
276.95	2.02
277.85	2.20
278.05	2.31
278.45	2.40
278.75	2.54
279.75	2.80
280.15	3.00
281.05	3.30
281.25	3.50
282.25	4.00

L_w – H – L_c	
T (°K)	P (MPa)
282.95	4.55
283.05	5.00
283.15	6.00
283.45	7.55
283.55	10.0
284.15	15.10
284.55	20.00
285.15	25.18
285.45	30.0
286.05	35.24
286.45	40.27
286.75	45.30
287.15	50.34
287.45	55.37
287.75	60.40
288.05	65.43
288.35	68.45

L_w – I – V	
T (C)	P (bar)
271.75	0.80
272.15	0.60
272.25	0.40
272.35	0.20

Estimated uncertainties: ±0.2 K (temperatures) and ±0.03 MPa (pressures below 30 MPa).

References

[1] P. Englezos, Technology readiness level of gas hydrate technologies, The Canadian Journal of Chemical Engineering 101 (2023) 3034–3043. URL: https://onlinelibrary.wiley.com/doi/abs/10.1002/cjce.24673. doi:https://doi.org/10.1002/cjce.24673. arXiv:https://onlinelibrary.wiley.com/doi/pdf/10.1002/cjce.24673.

[2] A. Touil, D. Broseta, A. Desmedt, Gas hydrate crystallization in thin glass capillaries: Roles of supercooling and wettability, Langmuir 35 (2019) 12569–12581.

[3] V. Melnikov, A. Nesterov, A. Reshetnikov, V. Istomin, Metastable states during dissociation of carbon dioxide hydrates below 273k, Chemical Engineering Science 66 (2011) 73–77. URL: https://www.sciencedirect.com/science/article/pii/S0009250910005932. doi:https://doi.org/10.1016/j.ces.2010.10.007.

[4] E. D. Sloan Jr, C. A. Koh, Clathrate hydrates of natural gases, CRC press, 2007.

[5] K. Yasuda, R. Ohmura, Phase equilibrium for clathrate hydrates formed with methane, ethane, propane, or carbon dioxide at temperatures below the freezing point of water, Journal of Chemical & Engineering Data 53 (2008) 2182–2188. URL: https://doi.org/10.1021/je800396v. doi:10.1021/je800396v. arXiv:https://doi.org/10.1021/je800396v.

[6] L. Ruffine, J. Trusler, Phase behaviour of mixed-gas hydrate systems containing carbon dioxide, The Journal of Chemical Thermodynamics 42 (2010) 605–611. URL: https://www.sciencedirect.com/science/article/pii/S002196140900295X. doi:https://doi.org/10.1016/j.jct.2009.11.019.

[7] Y. Nema, R. Ohmura, I. Senaha, K. Yasuda, Quadruple point determination in carbon dioxide hydrate forming system, Fluid Phase Equilibria 441 (2017) 49–53. URL: https://www.sciencedirect.com/science/article/pii/S0378381216306100. doi:https://doi.org/10.1016/j.fluid.2016.12.014, 2016 Asian Thermophysical Properties Conference.

[8] Y. Li, A. M. Gambelli, F. Rossi, S. Mei, Effect of promoters on co2 hydrate formation: thermodynamic assessment and microscale raman spectroscopy/hydrate crystal morphology characterization analysis, Fluid Phase Equilibria 550 (2021) 113218. URL: https://www.sciencedirect.com/science/article/pii/S0378381221002818. doi:https://doi.org/10.1016/j.fluid.2021.113218.

[9] A. Semenov, R. Mendgaziev, A. Stoporev, V. Istomin, T. Tulegenov, M. Yarakhmedov, A. Novikov, V. Vinokurov, Direct measurement of the four-phase equilibrium coexistence vapor–aqueous solution–ice–gas hydrate in water–carbon dioxide system, International Journal of Molecular Sciences 24 (2023). URL: https://www.mdpi.com/1422-0067/24/11/9321. doi:10.3390/ijms24119321.

[10] Y. Li, A. Maria Gambelli, J. Chen, Z. Yin, F. Rossi, E. Tronconi, S. Mei, Experimental study on the competition between carbon dioxide hydrate and ice below the freezing point, Chemical Engineering Science 268 (2023) 118426. URL: https://www.sciencedirect.com/science/article/pii/S0009250922010119. doi:https://doi.org/10.1016/j.ces.2022.118426.

[11] B. Samar, S. Venet, A. Desmedt, D. Broseta, Growth kinetics and porous structure of surfactant-promoted gas hydrate, ACS Omega 9 (2024) 31842–31854. URL: https://doi.org/10.1021/acsomega.4c03251. doi:10.1021/acsomega.4c03251. arXiv:https://doi.org/10.1021/acsomega.4c03251.

[12] A. Touil, D. Broseta, N. Hobeika, R. Brown, Roles of wettability and supercooling in the spreading of cyclopentane hydrate over a substrate, Langmuir 33 (2017) 10965–10977. URL: https://doi.org/10.1021/acs.langmuir.7b02121. doi:10.1021/acs.langmuir.7b02121. arXiv:https://doi.org/10.1021/acs.langmuir.7b02121, pMID: 28910532.

[13] Y. Li, A. M. Gambelli, F. Rossi, S. Mei, Effect of promoters on co2 hydrate formation: thermodynamic assessment and microscale raman spectroscopy/hydrate crystal morphology characterization analysis, Fluid Phase Equilibria 550 (2021) 113218. URL: https://www.sciencedirect.com/science/article/pii/S0378381221002818. doi:https://doi.org/10.1016/j.fluid.2021.113218.

[14] K. Ohgaki, Y. Makihara, K. Takano, Formation of co₂ hydrate in pure and sea waters, JOURNAL OF CHEMICAL ENGINEERING OF JAPAN 26 (1993) 558–564. doi:10.1252/jcej.26.558.

[15] J. W. Hedenquist, R. W. Henley, The importance of co 2 on freezing point measurements of fluid inclusions; evidence from active geothermal systems and implications for epithermal ore deposition, Economic Geology 80 (1985) 1379–1406. URL: https://doi.org/10.2113/gsecongeo.80.5.1379. doi:10.2113/gsecongeo.80.5.1379. arXiv:https://pubs.geoscienceworld.org/segweb/economicgeology/article-pdf/80/5

[16] L. W. Diamond, N. N. Akinfiev, Solubility of co2 in water from â^'1.5 to 100 Â°c and from 0.1 to 100 mpa: evaluation of literature data and thermodynamic modelling, Fluid Phase Equilibria 208 (2003) 265–290. URL: https://www.sciencedirect.com/science/article/pii/S0378381203000414. doi:https://doi.org/10.1016/S0378-3812(03)00041-4.

[17] V. Melnikov, A. Nesterov, L. Pendenko, A. Reshetnikov, Influence of carbon dioxide on melting of underground ice, Doklady Earth Sciences 459 (2014) 1353–1355. doi:10.1134/S1028334X14110245.

Declaration of interests

☒ The authors declare that they have no known competing financial interests or personal relationships that could have appeared to influence the work reported in this paper.

☐ The authors declare the following financial interests/personal relationships which may be considered as potential competing interests: